Specialization project

Jonas Bueie

2021

Contents

1 Summary

This project tests the Enskog-Thorne expression for the viscosity of a fluid mixture consisting of two different hard sphere fluids. Using molecular dynamics, such fluid mixtures has been simulated, and their shear viscosity has been measured. The results show agreement between simulations and Thorne's equation for the viscosity of hard sphere fluids.

2 Introduction

3 Literature review

4 Theory

4.1 Kinetic theory

4.2 Hard-sphere fluids

Hard-sphere (HS) fluids are fluids consisting of spherical particles interacting via the non-continuous potential

$$u(r) = \begin{cases} \infty, & r < \sigma \\ 0, & r > \sigma. \end{cases}$$

u is the interaction potential between two particles, r is the distance between them, and σ is the diameter of the particles. This potential makes it possible to analytically describe certain fluid properties using statistical mechanics. The HS potential is especially useful when modeling transport properties such as viscosity.

4.3 Transport properties

4.4 The viscosity of hard-sphere fluids

One expression for the viscosity of HS fluids is the Enskog equation. This equation applies to one-component HS fluids consisting only of particles with the same mass m and radius σ. The viscosity of such fluids is (Di Pippo et al. 1977)

$$\eta(\rho, T) = \eta_0 \left[g^{-1}(\sigma) + 0.8\, V_{\text{excl}}\, \rho + 0.776\, V_{\text{excl}}^2\, \rho^2 g(\sigma) \right].$$

Here,

$$\eta_0 = \eta(0, T) = \frac{5}{16\sigma^2} \sqrt{\frac{m\mathrm{k}T}{\pi}}$$

is the viscosity of the fluid in the zero-density limit. V_{excl}, the excluded volume, is the part of the fluid which a particle cannot occupy, because it is occupied by other particles. V_{excl} is commonly assumed to be the volume of all particles in the fluid. This however, is only correct in the zero-density limit. The space in between particles may also be unavailable.

Lastly, in equation (4.4), $g(\sigma)$ is a radial distribution function at contact. $g(\sigma)$ is the probability distribution of particles around one particle in the fluid. This determines how the collision frequency depends on the density of the fluid. $g(\sigma)$ can be found for example using the system's equation of state, as done in (ibid.). This method is referred to as Modified Enskog Theory.

In Enskog theory, a central assumption is that there is no correlation between different collisions. This assumption is known as molecular chaos. This means that the mean free time between collisions is much larger than the collision duration. The assumption of molecular chaos breaks down at high fluid densities, when collisions are too frequent to be uncorrelated. Furthermore, it does not work for real fluids with long range continuous interaction potentials, since long range interactions make the particles highly correlated. However, the assumption of molecular chaos is more acceptable for low density HS-fluids.

4.5 Viscosity of hard-sphere fluid mixtures

The Enskog equation (equation (4.4)) was generalized by Thorne to describe two-component fluid mixtures(Chapman et al. 1953). A further generalization to mixtures of arbitrary component numbers has been performed by Tham and Gubbins(Tham et al. 1971). The results are outlined below, as presented in (Di Pippo et al. 1977).

The viscosity of a dense binary mixture of two hard-sphere fluids is given by

$$\eta_{\text{mix}} = \left(\frac{y_1^2}{H_{11}} + \frac{y_2^2}{H_{22}} - \frac{2y_1 y_2 H_{12}}{H_{11}H_{22}} \right) \left(1 - \frac{H_{12}^2}{H_{11}H_{22}} \right)^{-1} + \frac{3}{5}\bar{\omega}_{\text{mix}},$$

where

$$y_1 = x_1 \left(1 + \frac{1}{2} x_1 \alpha_{11} \chi_{11} n + \frac{m_2}{m_1 + m_2} x_2 \alpha_{12} \chi_{12} n \right),$$

and

$$H_{12} = H_{21} = -\frac{2x_1 x_2 \chi_{12}}{\eta_{12}^0} \cdot \frac{m_1 m_2}{(m_1 + m_2)^2} \left(\frac{5}{3A_{12}^*} - 1 \right),$$
$$H_{11} = -\frac{x_1^2 \chi_{11}}{\eta_1^0} + \frac{2x_1 x_2 \chi_{12}}{\eta_{12}^0} \cdot \frac{m_1 m_2}{(m_1 + m_2)^2} \left(\frac{5}{3A_{12}^*} + \frac{m_2}{m_1} \right).$$

y_2 and H_{22} follow from exchanging the subscripts in y_1 and H_{11} respectively. A_{12}^* is a dimensionless ratio of collision integrals (of type ij). For hard spheres, A_{12}^* is exactly unity, and for other forms of interaction, it is close to unity.

$\chi_{ij} = \chi_{ji}$ are radial distrubution functions for molecules of type i colliding with molecules of type j. They correspond to the one-component radial distribution function $g(\sigma)$ in equation (4.4). Finally, $\bar{\omega}_{\text{mix}}$ can be written

$$\bar{\omega}_{\text{mix}} = x_1^2 \bar{\omega}_{11} + x_1 x_2 \bar{\omega}_{12} + x_2^2 \bar{\omega}_{22}, \text{where}$$
$$\bar{\omega}_{ij} = \frac{4}{9} n^2 \sigma_{ij}^4 \chi_{ij} \sqrt{\frac{2\pi m_1 m_2 \text{k} T}{m_1 + m_2}} \text{for} i, j = 1, 2.$$

It is instructive to demonstrate how the two-component Thorne equation (4.5) reduces to the one-component Enskog equation (4.4). This is done by setting the density of either of the components to zero. Setting $x_2 = 0$, so that $y_2, \omega_{\text{mix}} = x_1^2 om\bar{e}ga_{11}$ gives

$$H_{ij} = \begin{bmatrix} H_{11} & 0 \\ 0 & 0 \end{bmatrix}.$$

Now, equation (4.5) reduces to

$$\eta_{\text{mix}} = \frac{y_1^2}{H_{11}} + \frac{3}{5}\bar{\omega}_{\text{mix}} = \frac{\eta_1^0}{\chi_{11}}\left(1 + \frac{1}{2}x_1\alpha_{11}\chi_{11}n\right)^2 + x_1^2\bar{\omega}_{11}$$

Renaming the factors, this equals

$$\begin{aligned}\eta_{\text{one}} &= \frac{\eta^0}{g(\sigma)}\left[1 + \frac{1}{2}\alpha g(\sigma)\rho\right]^2 + x^2\bar{\omega} \\ &= \eta^0\left[g^{-1}(\sigma) + \frac{1}{2}\alpha\rho + \frac{1}{4}\alpha^2 g(\sigma)\right] + x^2\bar{\omega},\end{aligned}$$

Lastly,

$$\begin{aligned}\alpha &= \frac{8}{15}\pi\sigma^3, \quad \text{and} \\ \bar{\omega} &= \frac{4}{9}\rho^2\sigma^4 g(\sigma)\sqrt{\pi m \mathrm{k}T}\end{aligned}$$

is inserted, and it is assumed that $V_{\text{excl}} = \frac{N\pi\sigma^3}{6}$ is the total volume of the particles in the fluid. This gives equation (4.4)

$$\eta = \eta_0\left[g^{-1}(\sigma) + 0.8\, V_{\text{excl}}\,\rho + 0.776\, V_{\text{excl}}^2\,\rho^2 g(\sigma)\right].$$

4.6 Simulation of hard-sphere fluids

Several methods exist for simulating fluids consisting of rigid spheres. They can be divided into two categories, namely Monte Carlo (MC) models, and molecular dynamics (MD) models. MC methods sample statistical ensembles using random walk, while MD methods use Newton's equations of motion to compute the deterministic path of a large collection of particles.

Monte Carlo methods are typically easier to use with hard-sphere potentials, but can not be used to compute transport coefficients. Molecular dynamics methods on the other hand, allow calculating dynamical and out-of-equilibrium properties of a system. To compute the viscosity of a system, MD methods should therefore be used.

This section therefore gives an introduction to molecular dynamics, focusing especially on molecular dynamics for hard and pseudo-hard spheres (Allen et al. 1989).

4.7 Event-driven molecular dynamics simulation

A simple method for performing molecular dynamics simulations with hard sphere in is an *event-driven simulation*. Key elements of this simulation method is outlined below.

Compute the time until a collision occurs, for all particles in the system. All collisions are stored in a list containing at least information about the time of the collision, and the identity of the two involved particles. Then, the time until the earliest collision

is identified by searching through the list. Using Newton's equations of motion, all atoms are propagated freely until the collision happens. Through conservation laws, the colliding particles' velocities are then updated. Their next collisions are then added to the list of upcoming collisions. This process is repeated, and all atom positions are updated with the time until the next collision in the list.

It should be noted that after a collision happens, other collisions involving either of the two particles will be invalid. These should be discarded from the list.

4.8 Continuous potential MD simulation methods

Several powerful and efficient molecular dynamics programmes are easily available, including LAMMPS, GROMACS, DL_POLY and NAND. These do, however, not handle discontinuous potentials. Thus, the event-driven method is not supported by any of these programmes (Allen et al. 1989). In order to utilize the efficiency of the available MD software, it is more convenient to use a different method. The hard sphere potential can be approximated with a steep but continuous interaction potential instead. Then, the particle positions are updated using numerical integration methods with short, finite time steps.

Additionally, once there are long-range interaction forces between particles, then interactions occur at all times. In this case, the event driven simulation does not work, and integration methods are required. Therefore, continuous potential modelling is much more useful for realistic fluid models.

Several potentials are possible to use as hard-sphere approximations. The Lennard-Jones potential

$$u_{\mathrm{LJ}}(r) = 4\epsilon \left[\left(\frac{\sigma}{r}\right)^{12} - \left(\frac{\sigma}{r}\right)^{6} \right]$$

is a well-known example of historical importance. Here, ϵ is the well depth – the minimal value of the potential. As in (4.2), σ and r are the diameter and relative distance of the interacting particles.

If the attractive part, $\left[-\left(\frac{\sigma}{r}\right)^{6} \right]$ in equation (4.8) is removed from the potential, then $u_{\mathrm{LJ}}(r)$ can represent purely repulsive interactions. This is done by shifting the potential upwards by its minimal value ϵ and cutting it off there. Thus, the potential is exactly zero once it has reached its minimum. The resulting potential

$$u_{WCA}(r) = \begin{cases} 4\epsilon \left[\left(\frac{\sigma}{r}\right)^{12} - \left(\frac{\sigma}{r}\right)^{6} \right] + \epsilon, & r < 2^{\frac{1}{6}}\sigma \\ 0, & r > 2^{\frac{1}{6}}\sigma. \end{cases}$$

is known as a WCA-potential. This serves as an approximation to a hard sphere potential.

Increased computer efficiency makes it more appropriate to use steeper potentials than the WCA-potential. In particular, Jover et al. (Jover et al. 2012) has proposed the Mie

(or generalized Lennard-Jones) potential

$$u_{\text{Mie}}(r) = \frac{\lambda_r}{\lambda_r - \lambda_a} \left(\frac{\lambda_r}{\lambda_a}\right)^{\frac{\lambda_a}{\lambda_r - \lambda_a}} \epsilon \left[\left(\frac{\sigma}{r}\right)^{\lambda_r} - \left(\frac{\sigma}{r}\right)^{\lambda_a}\right],$$

as an approximation to the hard-sphere interaction potential. The exponents λ_r and λ_a define the strength of the repulsive and attractive parts of the potential.

Cutting and shifting the u_{Mie} potential as done in equations (4.8) and (4.8), gives a steep non-negative potential of the form

$$u_{(\lambda_a,\lambda_b)}(r) = \begin{cases} \frac{\lambda_r}{\lambda_r - \lambda_a} \left(\frac{\lambda_r}{\lambda_a}\right)^{\frac{\lambda_a}{\lambda_r - \lambda_a}} \epsilon \left[\left(\frac{\sigma}{r}\right)^{\lambda_r} - \left(\frac{\sigma}{r}\right)^{\lambda_a}\right] + \epsilon, & r < \sigma \left(\frac{\lambda_r}{\lambda_a}\right)^{\frac{1}{\lambda_r - \lambda_a}} \\ 0, & r > \sigma \left(\frac{\lambda_r}{\lambda_a}\right)^{\frac{1}{\lambda_r - \lambda_a}}, \end{cases}$$

closely resembling that of an infinitely steep hard wall potential (equation (4.2)). This potential is referred to as a pseudo hard-sphere (PHS) potential.

Jover et al. chose the exponents $(\lambda_r, \lambda_a) = (50, 49)$, as a compromise between faithfulness of the pseudo hard representation towards the perfectly hard wall, and computational speed. Higher exponents will produce a steeper repulsion. This however, comes at a cost. The steeper the potential, the shorter time steps are needed to ensure that the computations are precise. Therefore, steeper repulsions are computationally more expensive to simulate.

Writing it out for clarity, the Mie (50, 49)-potential has the form

$$u_{(50,49)}(r) = \begin{cases} 50 \left(\frac{50}{49}\right)^{49} \epsilon \left[\left(\frac{\sigma}{r}\right)^{50} - \left(\frac{\sigma}{r}\right)^{49}\right] + \epsilon, & r < \frac{50}{49}\sigma \\ 0, & r > \frac{50}{49}\sigma. \end{cases}$$

Pousaneh and de Wijn (Pousaneh et al. 2020) have shown that such a pseudo-hard sphere potential can be used to model viscosity for a one-component hard-sphere fluid, and that the obtained viscosity is in agreement with Enskog theory.

4.9 Measuring the viscosity of a fluid in NEMD

Müller-Plathe (Müller-Plathe 1999) has proposed a method of computing the viscosity of a fluid in nonequilibrium molecular dynamics (NEMD) simulations.

Consider a rectangular box with sides of length (L_x, L_y, L_z) with periodic boundary conditions. The box contains a hard sphere fluid at equilibrium. We divide the system into two equal slabs, their border being parallel to the xy-plane at height $z = L_z/2$. Now, we can define three parallel planes, at $z = \{0, L_z/2, L_z\}$, which are the edges of the two slabs. At these edges, we will control the velocity of the particles, making sure that the particles flow in the directions

$$\hat{u}_x(z) = \begin{cases} +\hat{x}, \; z = L_z, \\ -\hat{x}, \; z = L_z/2, \\ +\hat{x}, \; z = 0, \end{cases}$$

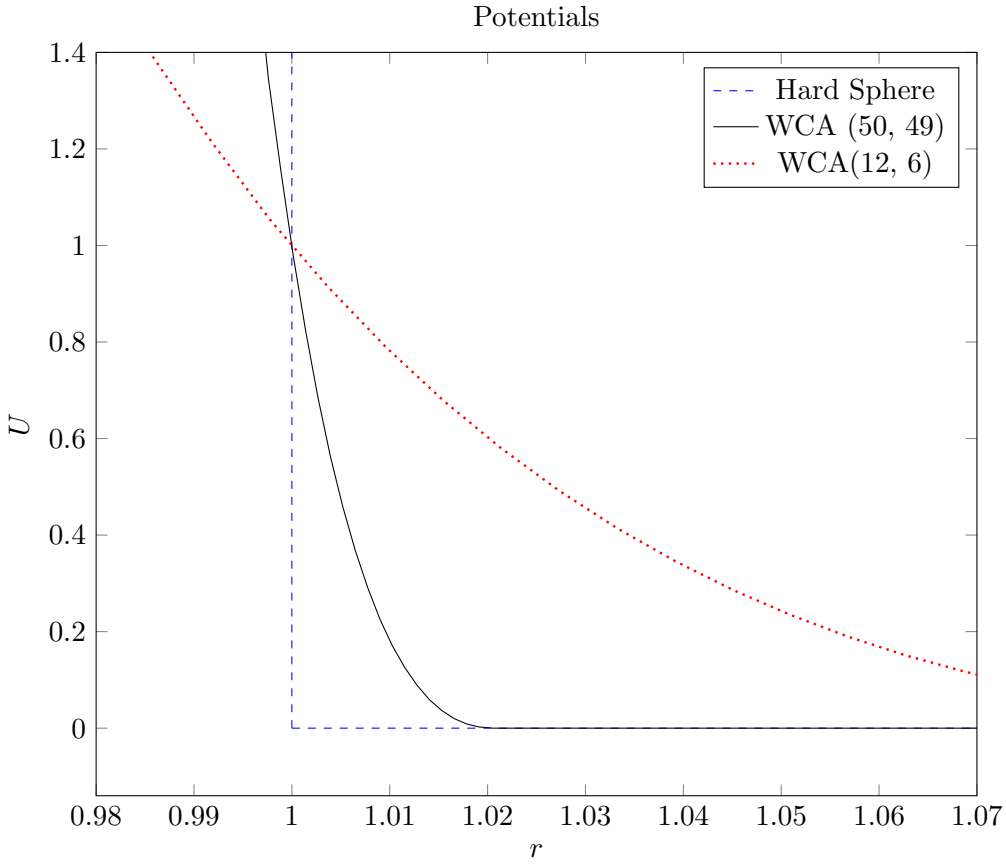

Figure 4.1: The cut-and-shifted WCA(50, 49)-potential compared to the cut and shifted WCA(12, 6) (Lennard-Jones) as well as the hard sphere potential.

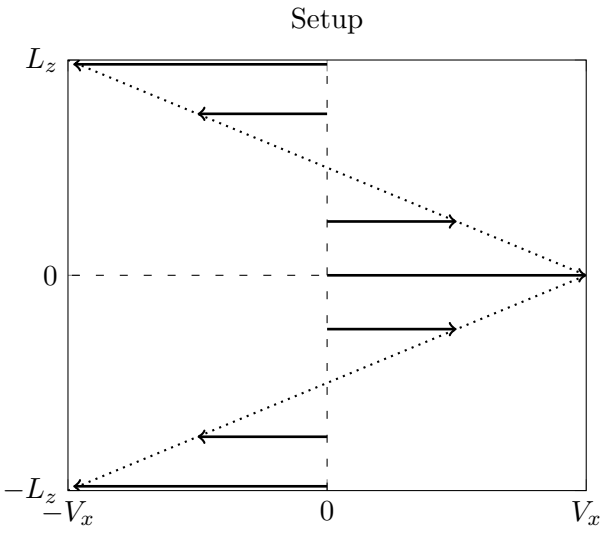

Figure 4.2: The setup of the Müller-Plathe experiment.

as shown in figure (??). Here, $u_x(z)$ denotes the average velocity component in x-direction, of the particles at height z. The hat "ˆ" denotes directional vectors of length unity.

The particle flows are adjusted through an unphysical process known as a **reverse perturbation**(Müller-Plathe 1999), as follows:

Find the particle in the $z = 0$ slab edge with the lowest (most negative) velocity component in the $+x$-direction. Correspondingly, find the particle in the $z = L/2$ border with the largest velocity component in the $+x$-direction. Then, swap the momenta of these two particles. Repeat the process for the top slab, swapping the smallest momentum in the $z = L$ edge with the largest momentum in the $z = L/2$ edge. This process is then repeated periodically. The repeated reverse perturbations cause a velocity profile in the fluid, as shown in figure (??). At the edges of the slabs, the velocity directions is given by equation (4.9).

The velocity profile will cause a momentum flux in z-direction,

$$j_z = -\eta \frac{\partial u_x}{\partial z}.$$

This flux is proportional to the viscosity of the fluid, and is measurable. Thus, the viscosity can be calculated from velocity data generated in the MD simulation.

5 Results

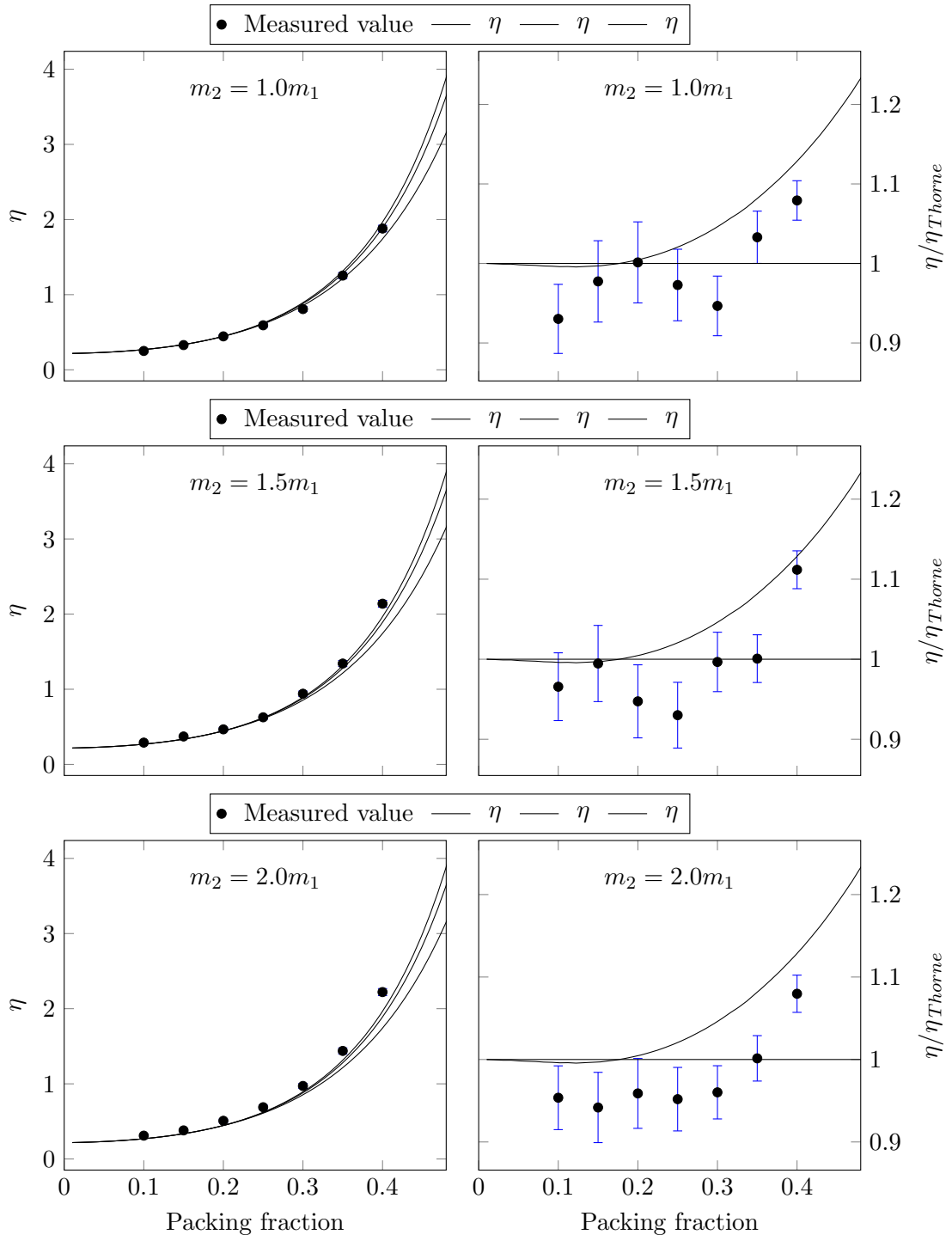

Figure 5.1: Measured viscosity for $m_2 = \{1.0m_1, 1.5m_1, 2.0m_1\}$

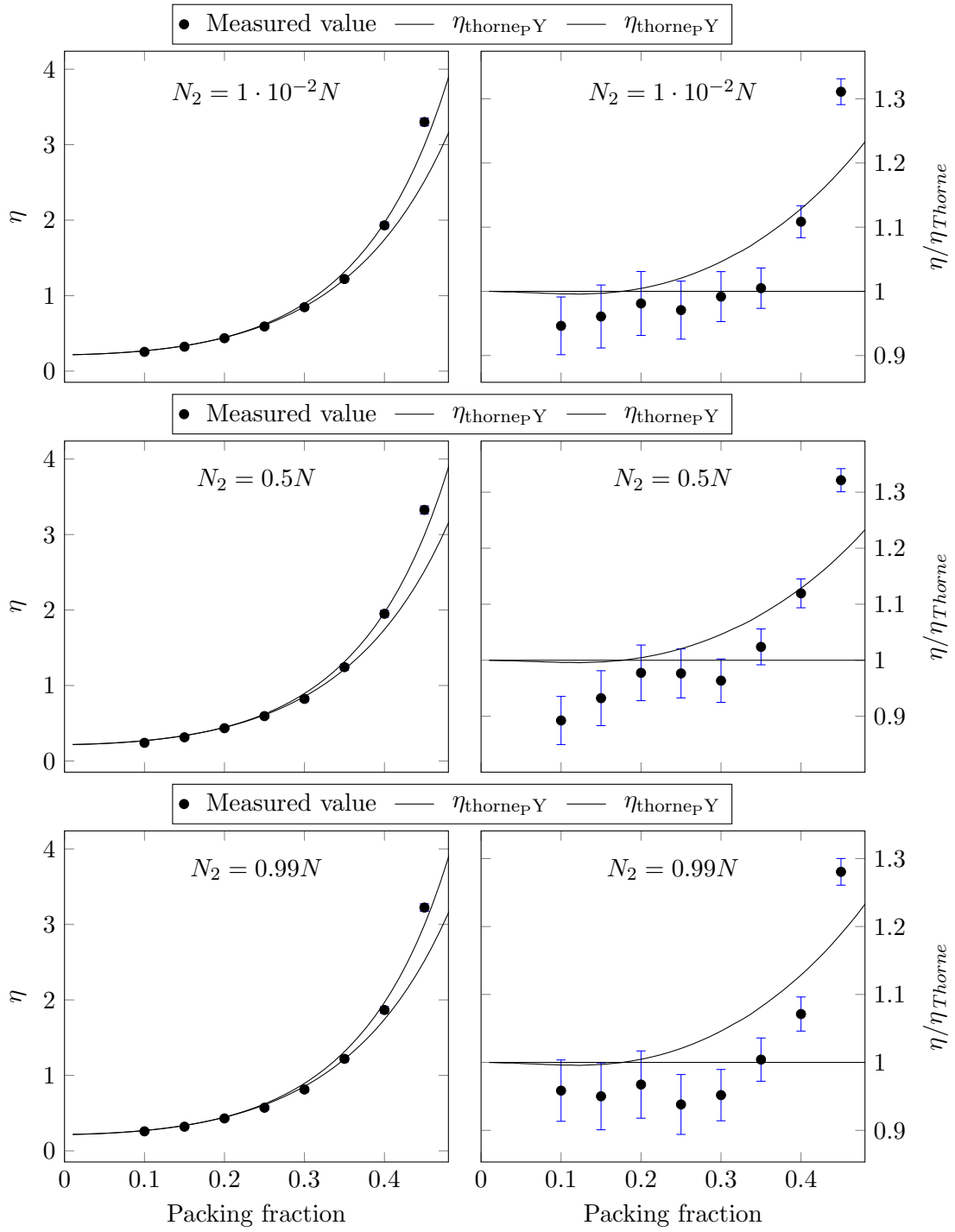

Figure 5.2: Measured viscosity for $N_2 = \{0.01N, 0.5N, 0.99N\}$

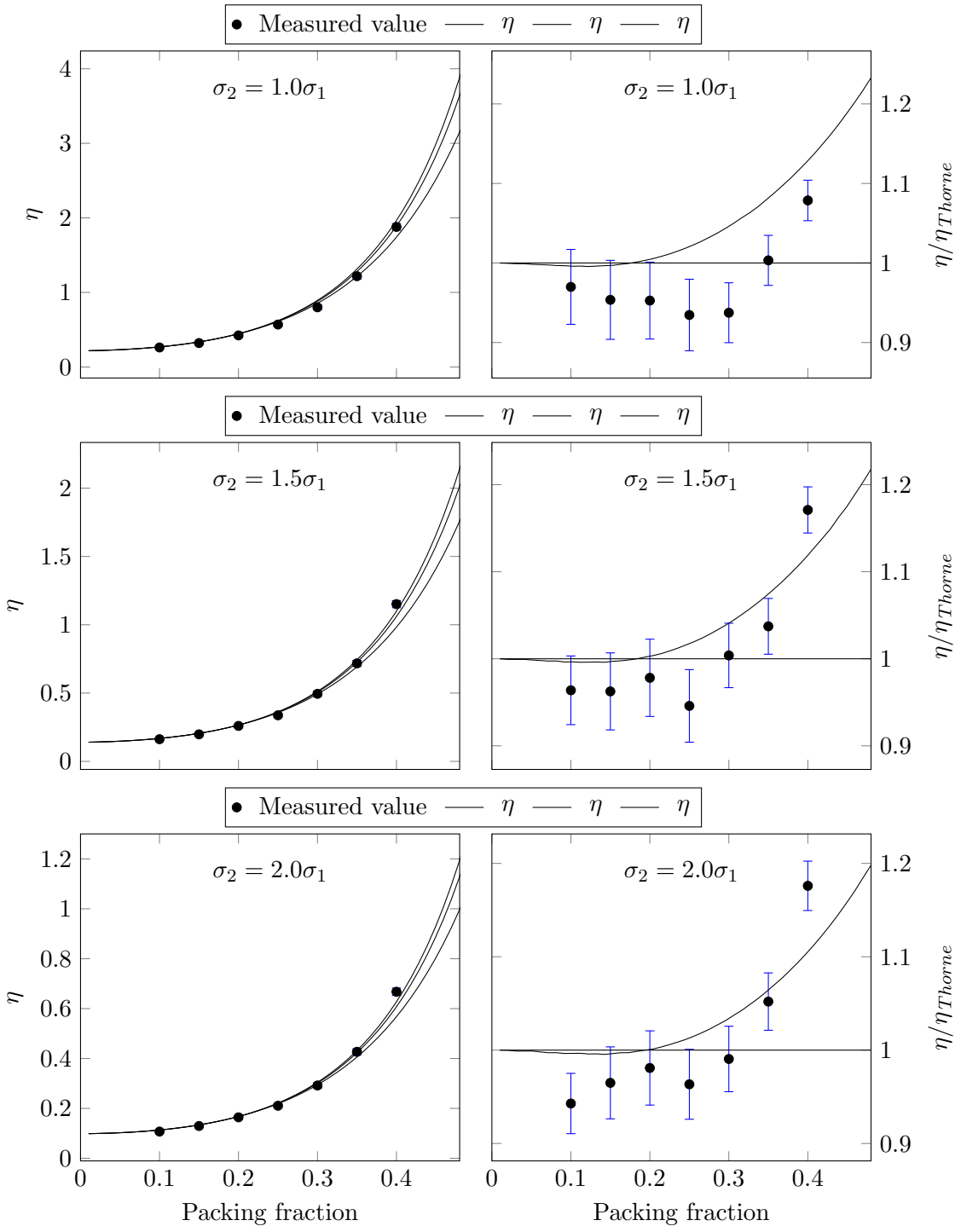

Figure 5.3: Measured viscosity for $\sigma_2 = \{1.0\sigma_1, 1.5\sigma_1, 2.0\sigma_1\}$

6 Discussion

7 Conclusion

Bibliography

Allen, M.P., D. Frenkel, and J. Talbot (1989). "Molecular dynamics simulation using hard particles". In: *Computer Physics Reports* 9.6, pp. 301–353. ISSN: 0167-7977. DOI: https://doi.org/10.1016/0167-7977(89)90009-9. URL: https://www.sciencedirect.com/science/article/pii/0167797789900099.

Chapman, S. and T. G. Cowling (1953). *The Mathematical Theory of Non-Uniform Gases*. 2nd ed.

Di Pippo, R. et al. (1977). "Composition dependence of the viscosity of dense gas mixtures". In: *Physica A: Statistical Mechanics and its Applications* 86.2, pp. 205–223. ISSN: 0378-4371. DOI: https://doi.org/10.1016/0378-4371(77)90029-2. URL: https://www.sciencedirect.com/science/article/pii/0378437177900292.

Jover, J. et al. (2012). "Pseudo hard-sphere potential for use in continuous molecular-dynamics simulation of spherical and chain molecules". In: *The Journal of Chemical Physics* 137.14, p. 144505. DOI: 10.1063/1.4754275. eprint: https://doi.org/10.1063/1.4754275. URL: https://doi.org/10.1063/1.4754275.

Müller-Plathe, Florian (May 1999). "Reversing the perturbation in nonequilibrium molecular dynamics: An easy way to calculate the shear viscosity of fluids". In: *Phys. Rev. E* 59 (5), pp. 4894–4898. DOI: 10.1103/PhysRevE.59.4894. URL: https://link.aps.org/doi/10.1103/PhysRevE.59.4894.

Pousaneh, Faezeh and Astrid S. de Wijn (2020). "Shear viscosity of pseudo hard-spheres". In: *Molecular Physics* 118.4, p. 1622050. DOI: 10.1080/00268976.2019.1622050. eprint: https://doi.org/10.1080/00268976.2019.1622050. URL: https://doi.org/10.1080/00268976.2019.1622050.

Tham, M. K. and K. E. Gubbins (1971). "Kinetic Theory of Multicomponent Dense Fluid Mixtures of Rigid Spheres". In: *The Journal of Chemical Physics* 55.1, pp. 268–279. DOI: 10.1063/1.1675518. eprint: https://doi.org/10.1063/1.1675518. URL: https://doi.org/10.1063/1.1675518.